Mesenchymal stem cells induce the ramification of microglia via the small RhoGTPases Cdc42 and Rac1

Veronika E. Neubrand, Marta Pedreño, Marta Caro, Irene Forte-Lago, Mario Delgado and Elena Gonzalez-Rey

Instituto de Parasitología y Biomedicina López-Neyra, IPBLN-CSIC, Avda. Conocimiento, PT Ciencias de la Salud, 18016 Granada, Spain

Corresponding Author: Elena Gonzalez-Rey, Instituto de Parasitología y Biomedicina López-Neyra, IPBLN-CSIC, Avd. Conocimiento, PT Ciencias de la Salud, 18016 Granada, Spain. Phone: 34-958-181670. Fax: 34-958-181632. email: elenag@ipb.csic.es

Running title: Cdc42 and Rac1 regulate the ramification of microglia

Word count: Abstract (248); Introduction (532); Materials and Methods (1884); Results (1411); Discussion (948); Acknowledgements (49); References (1101); Figure Legends (904). Total word count: 7249. Number of figures: 5.

Main points: Adipose-tissue derived mesenchymal stem cells induced microglia ramification, which was CSF-1 dependent and associated with anti-inflammatory, neuroprotective properties. The small RhoGTPases Rac1 and Cdc42 played a fundamental role in this process.

Key words: cell shape, neurodegeneration, neuroinflammation, colony stimulating factor-1

Abstract

Activated microglia play a central role in the course of neurodegenerative diseases, as they secrete cytotoxic substances which lead to neuronal cell death. Understanding the mechanisms that drive activation of microglia is essential to reverse this phenotype and to protect from neurodegeneration. With some exceptions, evidence indicates that changes in cell morphology from a star shape to a round and flat shape accompany the process of activation in microglia. In this study, we investigated the effect of adipose-tissue derived mesenchymal stem cells (ASCs), which exert important anti-inflammatory actions, in microglia morphology. Microglia exposed to ASCs or their secreted factors (conditioned medium) underwent a cell shape change into a ramifying morphology in basal and inflammatory conditions, similar to that observed in microglia found in healthy brain. Colony-stimulating factor-1 secreted by ASCs played a critical role in the induction of this phenotype. Importantly, ASCs reversed the activated round phenotype induced in microglia by bacterial endotoxins. The ramifying morphology of microglia induced by ASCs was associated with a decrease of the pro-inflammatory cytokines TNFα and IL6, an increase in phagocytic activity, and the upregulation of neurotrophic factors and of Arginase-1, a marker for M2-like regulatory microglia. Moreover, activation of the phosphoinositide-3-kinase/Akt pathway and the RhoGTPases Rac1 and Cdc42 played a major role in the acquisition of this anti-inflammatory phenotype. Therefore, these RhoGTPases emerge as key players in the ramification and deactivation of microglia by anti-inflammatory agents like ASCs, being fundamental to maintain the tissue-surveying, CNS supporting state of microglia in healthy conditions.

Introduction

Microglia are the resident immune cells of the central nervous system (CNS). They are activated once they detect any CNS lesion or dysfunction. During this activation process, microglia migrate to the insult site, secrete a variety of inflammatory cytokines and chemokines and perform phagocytosis (Jonas et al., 2012), similarly to classically activated macrophages (Mosser and Edwards, 2008). Since cytotoxic substances secreted by over-activated microglia lead to neuronal cell death, microglia play a central role in the course of neurodegenerative diseases, such as multiple sclerosis, Alzheimer's and Parkinson's diseases (Block et al., 2007). Therefore it is essential to understand the mechanisms of activation and de-activation processes at the molecular level, in order to limit a possible over-activation during neurodegenerative diseases and to return activated microglia back to non-inflammatory states, as they are found in a healthy CNS.

Interestingly, the activation of microglia can often be followed morphologically, since they change from a resting star-shaped form to a round and flat shape when activated (Hanisch and Kettenmann, 2007). However, this view has been revised recently (Perry et al., 2010). Because activated microglia can adopt many different phenotypes depending on the disease and other systemic influences, the morphology alone seems not to be sufficient to specifically identify these diverse phenotypes and functions. In this sense, some studies revealed that ramified microglia (historically characterized as "resting") can exert different functions and that microglia are able to respond without being morphologically activated (Cunningham et al., 2005). Therefore caution should be taken to directly infer function from preconceived morphological categories.

Nevertheless, any kind of morphological cell shape change underlies a rearrangement of the actin and microtubule cytoskeleton, which allows them to migrate to the site of

injury or inflammation and perform efficient phagocytosis (abd-el-Basset and Fedoroff, 1995; Cross and Woodroofe, 1999). The family of small RhoGTPases regulates these processes, but their role in microglia is largely unknown. Among the best characterized small RhoGTPases are Cdc42, which is involved in filopodia formation, and Rac1, being responsible for lamellipodia formation. Filopodia are actin bundles, ordered in a parallel manner, whereas lamellipodia are crosslinked actin filaments forming a meshwork. Both structures are indispensable for a variety of cellular functions in different cell types, such as cell migration, neuronal outgrowth and dendritic spine development.

On the other hand, mesenchymal stem cells (MSCs) isolated from many adult tissues have recently emerged as potent immunomodulatory cells with therapeutic applications in regenerative medicine (Phinney and Prockop, 2007) and in the treatment of inflammatory and autoimmune disorders (Uccelli and Prockop, 2010). Thus, MSCs derived from bone marrow and adipose tissue were shown to ameliorate experimental autoimmune encephalomyelitis and protected neurons from neuroinflammation in experimental models of brain ischemia and brain injury (Constantin et al., 2009; Uccelli et al., 2011; Zappia et al., 2005; Zhang et al. 2005). Among their multimodal actions, MSCs seem to modulate microglia activation (Kim et al., 2009; Zhou et al., 2009), although the mechanisms involved are largely unknown.

In the present study, we exploited the potential anti-inflammatory properties of adipose-derived MSCs (ASCs) in glial cells to investigate their effect on the morphological changes that microglia undergo in healthy and inflammatory conditions and to identify the intracellular signalling factors involved in this process.

Materials and Methods

Cell isolation and cultures

Primary microglia were prepared from P0 to P2 newborn C57Bl/6 mice. Dissected brains were discarded of olfactory bulb, cerebellum, hindbrain and meninges and then homogenized in microglia growth medium consisting in DMEM (Invitrogen), supplemented with 10% foetal bovine serum (FBS, Gibco), 10 % horse serum and 1% penicillin/streptomycin (Gibco), using a Pasteur pipette. Brain homogenates were centrifuged and the resulting cells were plated in poly-D-lysine-coated flasks and incubated with microglia growth medium for 10-14 days at 37°C and 5 % CO_2. Microglia were harvested on a shaker for 3 h at 200 rpm and plated on poly-D-lysine-coated cover-slips at a density of 16,000 cells/cm^2 or tissue culture 6-well plates in microglia growth medium at a density of 33,000 cells/cm^2. After 24 h, microglia growth medium was removed and fresh mouse MesenCult growth medium (Stem Cell) supplemented with mouse mesenchymal supplement (Stem Cell), herein referred as control medium, or by ASC conditioned medium (CM) were added to plates. We did not observe any difference in growth or cell shape in microglia grown with control medium compared to the standard microglia culture medium (data not shown). To confirm the purity of the microglia culture, cells were stained with a rat anti-CD11b antibody (clone M1/70, BD Biosciences), a microglial marker (Kettenmann et al., 2011), mouse anti-GFAP antibody (Molecular Probes), a marker for astrocytes, mouse anti-βIII-tubulin antibody (Covance) as a neuronal marker and rabbit anti-Olig-2 antibody (Millipore) to stain oligodendrocyte precursor cells. As result we observed that our primary microglia cultures consisted out of 99 % CD11b positive cells with a contamination of less than 0.02 % cells of astrocytes and oligodendrocyte precursor cells. No neurons were identified in these cultures. Moreover, microglia were cultured

in control medium in the absence or presence of transwell inserts plated with ASCs (see below). When indicated, lipopolysaccharide (LPS, serotype 055:B05 at 0.1 μg/ml, Sigma) was added to the microglia culture.

ASCs were isolated from adipose tissue of adult C57Bl/6 mice as previously described (Anderson et al., 2013). These cells showed a fibroblast-like morphology and differentiation capacity to the adipocytic and osteocytic lineages, and expressed the phenotype MCH-II$^-$CD14$^-$CD18$^-$CD31$^-$CD34$^-$CD45$^-$CD80$^-$CD117$^-$CD144$^-$ CD13$^+$CD44$^+$CD29$^+$CD54$^+$CD73$^+$CD90$^+$ CD105$^+$CD106$^+$CD166$^+$. ASC (2 x 10^4) were plated in transwell inserts (Millipore), which were transferred to 24-well plates containing microglia plated on coverslips at a cell density of 16,000 cells/cm^2. Cells were cultured in control medium for 48 h and microglia were analyzed for their shapes as described below. To determine gene and protein expression, ASCs (2 x 10^5) were plated in 6-well transwell inserts and then co-cultured in control medium with microglia plated in 6-well plates at a cell density of 33,000 cells/cm^2. At different time points, inserts were removed and total RNA and proteins of microglia were isolated as described below. Cell supernatants were collected to determine the amounts of TNFα as described below.

ASC CM was collected from passage 2 until passage 6 of ASC cultures, which were plated at a cell density of 15,000 cells/cm^2, grown for 2 days before collecting their supernatant and then stored at -20°C. Before use, the ASC CM was quickly thawed and passed through a 0.2 μm filter. When indicated, ASC CM was depleted of various cytokines by incubating with anti-CSF-1 and anti-IL6 antibodies (10 μg/ml, both from BD Biosciences) for 20 min prior to its addition to microglia cultures.

In some experiments, microglia were incubated with the inhibitors PD 98059 (50 μM, Invitrogen) and LY 294002 (10 μM, Invitrogen) in microglia growth medium for

30 min, then the medium was removed and cells were incubated in ASC CM supplemented with the inhibitors at the same concentrations. After 24 h of culture, microglia were fixed and evaluated for cell shape as described below.

For transfection, microglia (1.2 x 10^5 cells in suspension) were nucleofected with plasmids expressing GFP-tagged wild-type and dominant negative mutants of Cdc42 and Rac1 (Estrach et al., 2002) using the Amaxa nucleofector Small Cell Number (SCN) Kit according to manufacturer's instructions with the SCN programme 6 and plated on cover-slips coated with poly-D-lysine in microglia growth medium. After 2 h, medium was replaced with fresh growth microglia medium. 24 h later, microglia were incubated with ASC CM for 48 h and analyzed for changes in cell shape. Although the transfection efficiency for GFP was 20%, it decreased to less than 0.1% for the GFP-tagged wild-type and dominant negative mutants of Cdc42 and Rac1.

Determination of cell shape and form factor

Microglia plated on cover-slips were fixed for 20 min in 3.5% paraformaldehyde, permeabilized in Triton X-100 and immunostained with the primary rat anti-CD11b antibody (clone M1/70, BD Biosciences) for 30 min at room temperature. After three washes with PBS, samples were incubated with Alexa Fluor488-conjugated secondary antibody (Molecular Probes) for 30 min at room temperature and then mounted with Mowiol (Sigma). Images were acquired with 10x, 40x or 60x objectives on an Olympus IX 81 fluorescence microscope. To determine the form factor, images were analyzed using Image J. Each image was processed by the median filter at a radius of 8 pixels, then a black and white threshold image was generated. Cell surroundings were drawn by the wand tracing tool and the area and the perimeter of each cell was determined. Cells touching the borders of the image were excluded from the quantification

procedure. The form factor was calculated using the formula 4π*area/(perimeter)^2 described previously (Wilms et al., 1997). Form factors close to 1 correspond to round cells and values approaching 0 indicate highly ramified cells. At least 102 cells per condition were analyzed in at least three independent experiments, except for the transfected cells (experiments showed in Figure 5 B), where due to the low transfection efficiency, 45 to 69 cells per mutant were analysed in four independent experiments.

ELISA

TNFα levels in culture supernatants were determined using a specific sandwich ELISA that uses capture/biotinylated detection antibodies from BD Pharmingen according to the manufacture's recommendations.

Western blot analysis

Microglia were grown in microglia growth medium, then the medium was changed to control medium (medium), control medium + LPS (LPS), ASC conditioned medium (CM), ASC conditioned medium + LPS (CM+LPS), ASC plated in transwell inserts (ASC) and ASC plated in transwell inserts + LPS (ASC+LPS) for the indicated time periods. For the detection of ADNP and BDNF, cells were incubated for 24h in 2 μM monensin (Sigma) in the indicated medium. Subsequently they were harvested with cold lysis buffer consisting in 10 mM Tris-HCl pH 8.0, 150 mM NaCl, 1% Nonidet-P40, 1 mM EDTA, 10 mM NaF, 1 mM Na_3VO_4, a cocktail of commercially available protease inhibitors (Sigma, containing 104 mM AEBSF, 80 μM Aprotinin, 4 mM Bestatin, 1.4 mM E-64, , 2 mM Leupeptin, 1.5 mM Pepstatin A) and phosphatase inhibitors (PhosStop from Roche, acting against a wide spectrum of phosphatases, including acid and alkaline phosphatases, serine/threonine phosphatases PP1, PP2A and

PP2B and tyrosine protein phosphatases PTP). After centrifugation for 15 min at 14,000 rpm, the protein concentration of the supernatants was determined by Bradford assay (Bio-Rad) and samples were prepared for SDS-PAGE with Laemmli SDS sample buffer. After semi-dry blotting, PVDF membranes were blocked with 5% BSA in TBS and incubated 8-10 h at 4ºC with the primary antibodies, including rabbit anti-Akt, rabbit anti-phospho-Akt, rabbit anti-Cdc42, rabbit anti-phospho-Erk1/2, rabbit anti-Erk1/2 (all from Cell Signalling), mouse anti-Rac1 (BD Transduction laboratories), mouse anti-Arginase-1 (BD Transduction Laboratories), rabbit anti-GAPDH (Sigma), rabbit anti-BDNF (Peprotech), rabbit anti-ADNP (Antibody-Online) or mouse anti-α-tubulin (Sigma) antibodies diluted in the blocking solution. Horseradish peroxidase-conjugated secondary antibodies (DakoCytomation) and ECL (GE Biotech) were used for detection. If necessary, membranes were stripped with stripping buffer (100 mM β-mercaptoethanol, 2 % SDS, 62.5 mM Tris pH 6.8) for 30 min at 55°C.

RNA extraction and qRT-PCR

Total RNA was extracted using Tripure (Roche) from microglia plated in 6-well plates. After DNase I treatment (Sigma), RNA (1 μg/sample) was reverse transcribed using RevertAid First Strand cDNA Synthesis kit (Fermentas) and random hexamer primers. The cDNA was analyzed by qPCR in triplicates on an i-Cycler (Bio-Rad) with the iQ^{TM} SYBR®Green Supermix (Bio-Rad) and 2.5 pmol of the following primers: mouse TNFα forward, AAC TAG TGG TGC CAG CCG AT; mouse TNFα reverse, CTT CAC AGA GCA ATG ACT CC; mouse β-actin forward, AAT CGT GCG TGA CAT CAA AG; mouse β-actin reverse, ATG CCA CAG GAT TCC ATA CC; mouse BDNF forward, CCC TCC CCC TTT TAA CTG AA; mouse BDNF reverse, GCC TTC ATG CAA CCG AAG TA; mouse ADNP forward, AGA AAA GCC CGG AAA ACT

GT; mouse ADNP reverse, AAG CAC TGC AGC AAA AAG GT; mouse IL6 forward, TGC TGG TGA CAA CCA CGG CCT; mouse IL6 reverse, GGC ATA AAC GCA CTA GGT TTG CCG A; mouse FGF2 forward, GCG ACC CAC ACG TCA AAC TA; mouse FGF2 reverse, CCG TCC ATC TTC CTT CAT AGC; mouse GDNF forward, TCC AAC TGG GGG TCT ACG G, mouse GDNF reverse, GCC ACG ACA TCC CAT AAC TTC AT. After 42 cycles, the Ct values were determined. To normalize the samples, ΔCt between the gene of interest and β-actin Ct values was calculated. The x-fold difference in expression between the different treatments was then determined by subtraction of the ΔCt values and called ΔΔCt. Finally, the total change was calculated as $2^{-\Delta\Delta ct}$ and the relative amount compared to medium-treated cells was deducted.

RhoGTPase activation assays

To determine Cdc42 and Rac1 activation, we performed a GST-pulldown using the CRIB domain of Pak1 as previously described (Briancon-Marjollet et al., 2008). Microglia were treated with the indicated conditions and scraped with ice-cold lysis buffer (25 mM Hepes-NaOH pH 7.5, 1% Nonidet-P40, 10 mM $MgCl_2$, 100 mM NaCl, 5% glycerol, 100 mM PMSF, phosphatase inhibitors (PhosStop from Roche)). Lysates were centrifuged for 30 s at 14,000 rpm, the supernatant incubated with 20 μg GST-CRIB beads for 30 min at 4°C and washed with binding buffer (25 mM Hepes-NaOH pH 7.5, 0.5% Nonidet-P40, 30 mM $MgCl_2$, 40 mM NaCl, 1 mM dithiothreitol). Finally, beads were resuspended in 12 μl of sample buffer, loaded on an SDS-PAGE together with 15 μl of the cell lysate to determine the total amount of Cdc42 or Rac1 per sample and analyzed by Western blot as described above.

Phagocytosis assay

Nile Red FluoSpheres (1 μm-diameter microspheres, Life Technologies) were washed in distilled water, pelleted (10,000 *g*, 15 min, room temperature) and coated by incubation in 3% BSA containing 20 mM sodium phosphate buffer pH 7.4 at room temperature for 15 min on a rotating wheel. Subsequently the microspheres were washed with the phosphate buffer containing 1% BSA and resuspended in the same buffer. Before starting the phagocytosis assay, the microspheres were opsonized with inactivated FBS (Gibco) for 1 h at 37°C and then added (10^9 microspheres/ml) to microglia. The microspheres were homogenously distributed throughout each well by gentle movements of the plate. After 1 h of incubation at 37°C, the medium containing non-phagocytosed microspheres was removed and the cells were washed twice with PBS prior to their fixation with 3.5% paraformaldehyde in PBS for 20 min at room temperature. The number of microglia that phagocytosed and the number of phagocytosed microspheres per cell were determined on an Olympus IX 81 fluorescence microscope.

Statistical analysis

All data are expressed as the mean±SEM. Statistical analysis was carried out with two-way ANOVA followed by Student's *t*-test. We assumed significance at $p<0.05$.

Results

ASCs induce microglia ramification

Because morphological changes in microglia cells can correlate with their activation state (Hanisch and Kettenmann, 2007; Kettenmann et al., 2011; Perry et al., 2010), we first investigated the immune-modulatory effect of ASCs on the cell shape of microglia in basal non-inflammatory conditions. After 48 h, cells were fixed and changes in microglia morphology were assessed by staining with the microglia marker CD11b (Figure 1A). To avoid cell-to-cell contact, ASCs and microglia were co-cultured in a transwell systems separated by a semipermeable membrane. The presence of ASCs in the culture induced a drastic change in the microglia shape, characterized by the appearance of spindle-like extensions (Figure 1A). The fact that we observed these effects in a transwell system suggested that soluble factors produced by ASCs might mediate the induction of microglia ramification. Indeed, conditioned medium (CM) collected from ASC cultures increased the ramification of microglia. Next, we evaluated whether the action of ASCs in microglia morphology was also observed in an inflammatory milieu. As previously reported (abd-el-Basset and Fedoroff, 1995; Wilms et al., 1997), the bacterial endotoxin LPS induced a round and flat shape in microglia, and both ASCs and their CM prevented this cell shape change (Figure 1A). Even more important was that ASC CM reversed the inflammatory phenotype acquired by microglia previously exposed to LPS (Figure 1B).

In summary and based on the criteria for morphological categories of microglia described by Karperien et al, 2013, we observed in our experiments three morphological types: 1) Cells that were grown in medium were classified as ramifying/bushy, which are characterized by numerous short and thick processes, arranged in thick bundles around swollen somata, hereafter called “bushy” microglia. 2) ASCs/CM induced a

ramifying/hypertrophied phenotype, which show frequently elongated, larger somata, thicker primary and retracting secondary processes, hereafter referred to as “ramifying” microglia. 3) LPS-stimulated microglia were unramified/amoeboid, bearing no processes with a large round to variable shaped cell body. Interestingly, in our *in vitro* experimental set-up, we did not observe the ramified complexity as usually seen *in vivo*, an observation also mentioned by others (Karperien et al., 2013; Kettenmann et al., 2011).

For the quantification of our results, we decided to use the form factor amongst other available methods (Karperien et al., 2013; Soltys et al., 2001), because it was previously shown that it discriminates well between bushy, hypertrophied and unramified cells (Soltys et al., 2001; Wilms et al., 1997). For example, a form factor with the value of 1 corresponds to a round cell, whereas values tending to 0 indicate ramified cells (Wilms et al., 1997). The quantification of our experiments with the form factor revealed that bushy medium-treated cells showed a value of 0.37±0.02, that unramified LPS-stimulated cells had a form factor of 0.47±0.02 and that the incubation with ASCs or their CM significantly reduced the form factor of microglia in both basal and inflammatory conditions (Figure 1).

The ASC-induced ramification of microglia is CSF-1 dependent.

The previous results indicate that the ramification of microglia was induced by a soluble factor secreted by the ASCs rather than direct cell-cell contact. Therefore, we next investigated whether some of the molecules secreted by ASCs, among them the colony stimulating factor-1 (CSF-1, also known as macrophage-CSF or M-CSF) and the cytokine interleukin 6 (IL-6) (M.D. unpublished data) were involved in microglia cell shape changes induced by ASCs. We found that the depletion of CSF-1, but not of IL-6,

in ASC CM reversed almost completely the induction of microglia ramification observed previously (Figure 2), suggesting a major involvement of CSF-1 produced by ASCs in the change of microglia morphology. Indeed, microglia cells treated with recombinant CSF-1 showed a ramifying phenotype and a decreased form factor (Figure 2). We also observed that indomethacin, an inhibitor of the cyclooxygenase enzyme responsible for the prostaglandin E2 production, did not affect the degree of ramification of ASC-treated microglia (data not shown), indicating that prostaglandin E2 is not essential for the ASC-induced microglia ramification.

Ramifying microglia induced by ASC showed a non-inflammatory phenotype

The initial hypothesis of our study is that ramified microglia exert anti-inflammatory functions as opposed to round pro-inflammatory microglia stimulated with LPS. Although the microglia shape might be an indicator of its function, the activation state of microglia should be confirmed by additional experiments. Therefore, we investigated whether, besides changes in microglia morphology, ASCs or their CM were able to regulate other factors related to the inflammatory response of microglia. Thus, we found that treatment with ASC CM prevented LPS-induced expression of the inflammatory cytokines IL-6 and TNFα in microglia (Figure 3A and B), suggesting that ASCs induce an anti-inflammatory state in microglia. We next tested whether the microglia generated in the presence of ASC CM were simply in a quiescent unresponsive state or whether they were able the produce factors involved in regenerative processes. Thus, we observed that microglia treated with ASC CM produced between 2.5- and 11-fold more neurotrophic and neuroprotective factors, such as activity-dependent neurotrophic protein (ADNP), brain-derived neurotrophic factor (BDNF) and basic fibroblast growth factor (FGF2) than microglia incubated with control medium (Figure 3C and D).

Although ASC CM alone did not affect the expression of glial cell-derived neurotrophic factor (GDNF) in microglia (Figure 3C), it avoided the LPS-induced decrease of this neurotrophic factor (36 % and 92 % GDNF expression compared to 100 % in medium-treated microglia for LPS- and LPS+CM-treated cells, respectively, p=0.04). Moreover, microglia cultured in the presence of ASCs or their CM were able to produce high levels of arginase-1, a marker for alternatively activated and anti-inflammatory macrophages (Munder, 2009), in both basal and inflammatory conditions (Figure 3E). Finally, we evaluated the phagocytic activity of microglia incubated with ASC and their CM. As Figure 3F shows, treatment with ASC and CM increased dramatically the phagocytic capacity of microglia for inert microspheres in comparison to microglia incubated with control medium (ASC and CM increased both the number of phagocytosing cells and the number of microspheres per cell). These data support the idea that ASC-treated microglia are not just in a quiescent state, but have rather activated a cell program promoting neuroprotective activities.

ASC CM induced signalling pathways involved in the regulation of microglia morphology

We next investigated the intracellular pathways that could be involved in the induction of the phenotype observed in microglia generated in the presence of ASC CM. Evidence from the literature indicates that the phosphoinositide-3-kinase (PI3K)/Akt-dependent signalling pathway promotes anti-inflammatory properties in microglia (Tarassishin et al., 2011), and stimulates actin polymerization and phagocytosis (Song et al., 2012). Moreover, the morphological change between different microglia phenotypes underlies a rearrangement of the actin cytoskeleton (abd-el-Basset and Fedoroff, 1995; Cross and Woodroofe, 1999), and the small RhoGTPases

Rac1 and Cdc42 regulate these processes. Furthermore, the activation of Rac1 and Cdc42 partially depends on the activity of PI3K. We found that treatment with ASC CM rapidly activated Akt (measured as its phosphorylated form) in microglia in both basal and inflammatory conditions (Figure 4A). Moreover, since CSF-1 activates not only the PI3K pathway, but also Extracellular-signal-Regulated Kinases 1/2 (ERK1/2) (Bourette and Rohrschneider, 2000; Pixley 2012) in macrophages and other cell types, in which ERK1/2 activation regulates lamellipodia formation and cell polarity, we tested whether this would be also the case in our experimental system. Indeed, we found a strong ERK1/2 phosphorylation upon ASC CM treatment in microglia (Figure 4A). By using a pull-down system to detect the GTP-bound active form of the RhoGTPases, we observed that ASC CM activated rapidly both Rac1 and Cdc42 GTPase activities, mainly in basal conditions (Figure 4B and 4C).

In order to confirm the involvement of these pathways in the phenotype induced in microglia by ASCs, we first inhibited the PI3K activity using LY 294002 and the ERK1/2 activity using the MEK inhibitor PD 98059 in ASC CM-treated microglia. Figure 5A shows that the PI3K/Akt inhibitor blocked significantly the microglia ramification induced by ASC CM. However, the MEK inhibitor only slightly reversed the effect of ASC CM (Figure 5A).

Moreover, we investigated the involvement of Cdc42 and Rac1 by nucleofecting microglia with dominant negative mutants (DN) of these RhoGTPases and then treated them with ASC CM. We observed that the expression of dominant negative mutants of Cdc42 and Rac1 inhibited the ramification of microglia induced by ASC CM (Figure 5B). These findings suggest that activation of PI3K/Akt, Cdc42 and Rac1 are essential for the generation of ramified, surveying microglia by ASCs and play a major role in the transition between activated and resting microglia.

Discussion

In a healthy brain, microglia are found in a highly ramified morphology, surveying and supporting continuously the surrounding tissue (Hanisch and Kettenmann, 2007). While it is now clear that any brain insult, inflammation or infection leads to microglia activation in order to secrete inflammatory factors, it has been less studied how or through which factors microglia can return to their originally ramified phenotype with their tissue supporting properties. Previous studies indicate that MSCs can influence microglia towards that direction (Kim et al., 2009; Zhou et al., 2009), but no detailed investigation on their morphology nor on intracellular molecules involved in the cell shape change has been performed. In this study, we showed that ASCs induce in microglia a cell shape change into a ramifying morphology, even in the presence of inflammatory stimuli. Noteworthy, ASCs were able to reverse the round, flat microglia phenotype acquired in an inflammatory milieu. Since we show in our study that ASCs were able to setback an inflammatory microglia phenotype into a ramifying, anti-inflammatory one, they are the ideal tool to study the molecular mechanism behind this reversion.

In agreement with its non-inflammatory supporting function, microglia exposed to ASCs did not express the pro-inflammatory cytokines TNFα and IL6, even in the presence of bacterial mediators of inflammation. Far to be in an unresponsive quiescence, the microglia generated by ASCs were in an active state characterized by the expression of neurotrophic factors and a strong phagocytic activity, which play an important role in the supportive activity of resting microglia in healthy CNS. Moreover, we found that ASCs induced the expression of Arginase-1 in microglia, a marker for alternatively-activated or regulatory macrophages, which downregulates inflammation during late stages of adaptive immunity (Mosser and Edwards, 2008). Although

microglia can adopt a variety of different phenotypes (Perry et al., 2010) and thus a classification in “M1” or “M2-like” microglia might not be correct, ASC treatment seems to generate a kind of anti-inflammatory regulatory or alternatively-activated microglia, which could be similar to “M2-like” microglia/macrophages as opposed to “M1-like” microglia/macrophages, representing classically activated microglia/macrophages with a pro-inflammatory profile (Mosser and Edwards, 2008). The induction of this phenotype in microglia in the CNS could play a major role in the protective effect shown by ASC-based treatments in many neurodegenerative disorders that course with neuroinflammation.

Consisting with previous studies, these cell shape changes are likely to be mediated via the signalling pathways initiated mainly by PI3K/Akt, and maybe by ERK1/2 (Song et al., 2012; Tarassishin et al., 2011). We also observed that the small RhoGTPases Rac1 and Cdc42 play a fundamental role in the ramification of microglia induced by ASCs. Both events, activation of PI3K and these small RhoGTPases, are probably related. In parallel to the activation of Akt, PI3K phosphorylates phospho-inositol, generating phosphatidylinositol-(3,4,5)-triphosphate (PIP3) (Hawkins et al., 2006), which is an important lipid mediator, recruiting proteins containing Pleckstrin-Homology (PH) domains to the membrane, such as Akt and PH domain containing Rho guanine nucleotide exchange factors (RhoGEFs), the activators of RhoGTPases (Rossman et al., 2005). Indeed, the prerequisite for a successful GDP exchange on small RhoGTPases is their membrane recruitment (Rossman et al., 2005). Thus, the generation of PIP3 is an important event in activating RhoGTPases via their corresponding RhoGEF. Once activated, Rac1 and Cdc42 can recruit their effector proteins (Ridley, 2011) and induce actin polymerization in the form of lamellipodia and filopodia, respectively. This actin polymerization would lead to drastic changes in the cell morphology, inducing the

ramification of microglia and stimulating their phagocytic activity. Like in neurons where both the actin cytoskeleton and signalling molecules act in concert for successful axonal and dendritic growth (Huber et al., 2003), it is likely that also in microglia a concerted action of actin remodelling and gene expression is necessary to generate ramifying, anti-inflammatory microglia.

Our study clearly demonstrates that the effect of ASCs on microglia shape is fully mediated by soluble trophic factors produced by the mesenchymal cells. Among the main factors produced by ASCs, we found that CSF-1 is necessary and sufficient for the induction of ramification in microglia, while IL-6 and prostaglandin E2, which were previously involved in the anti-inflammatory action of these cells (Anderson et al., 2013; Gonzalez-Rey et al., 2010), are not essential in this process. CSF-1, initially described as a major growth factor for macrophages (Pixley and Stanley, 2004), is now recognized as a cytokine that plays an essential role in the differentiation, growth and motility of microglia *in vitro* and *in vivo*. CSF-1 appears to be important for maintaining a normal number of microglial cells in the brain (Erblich et al., 2011; Giulian and Ingeman, 1988; Wegiel et al., 1998). In addition, CSF-1 was found to induce ramification of human fetal microglia in vitro (Liu et al., 1994). In macrophages and other cell types, binding of CSF-1 to its receptor leads to phosphorylation of PI3K and ERK1/2, and subsequently to activation of small RhoGTPases, to actin polymerization, changes in cell morphology and migration (Bourette and Rohrschneider, 2000; Lo et al., 2008; Martin et al., 2003; Pixley, 2012; Sampaio et al., 2011; Smith et al., 2008). These findings support our data describing that CSF-1 produced by ASCs is involved in the induction of the ramified morphology in microglia and links CSF-1 to the intracellular signalling observed during this process.

In summary, we provide for the first time a comprehensive study of the parameters that drive the microglial shape changes induced by MSCs, with the aim to elucidate the factors required to re-programme pro-inflammatory damage-inducing microglia back to their tissue-surveying, CNS supporting function. These factors represent possible drug-targets for the treatment of neurodegenerative diseases, in order to be able to prevent further neuronal cell death induced by inflammatory microglia.

Acknowledgements

We thank G. Robledo and J. Campos-Salinas (IPBLN, CSIC) for technical help in tissue culture and cell shape determination, respectively. This work was supported by the Spanish Ministry of Science and Innovation (JCI-2008-01843 to VN and grant number SAF2010-16923 to EG-R) and Excellence Grants of Andalusian Government (to M.D.).

Competing Financial Interest: Authors declare no competing financial interest.

References

abd-el-Basset E, Fedoroff S. 1995. Effect of bacterial wall lipopolysaccharide (LPS) on morphology, motility, and cytoskeletal organization of microglia in cultures. J Neurosci Res 41:222-237.

Anderson P, Souza-Moreira L, Morell M, Caro M, O'Valle F, Gonzalez-Rey E, Delgado M. 2013. Adipose-derived mesenchymal stromal cells induce immunomodulatory macrophages which protect from experimental colitis and sepsis. Gut 62:1131-1141.

Block ML, Zecca L, Hong JS. 2007. Microglia-mediated neurotoxicity: uncovering the molecular mechanisms. Nat Rev Neurosci 8:57-69.

Bourette RP, Rohrschneider LR. 2000. Early events in M-CSF receptor signaling. Growth Factors 17:155-166.

Briancon-Marjollet A, Ghogha A, Nawabi H, Triki I, Auziol C, Fromont S, Piche C, Enslen H, Chebli K, Cloutier JF, Castellani V, Debant A, Lamarche-Vane N. 2008. Trio mediates netrin-1-induced Rac1 activation in axon outgrowth and guidance. Mol Cell Biol 28:2314-2323.

Constantin G, Marconi S, Rossi B, Angiari S, Calderan L, Anghileri E, Gini B, Bach SD, Martinello M, Bifari F, Galiè M, Turano E, Budui S, Sbarbati A, Krampera M, Bonetti B. 2009. Adipose-derived mesenchymal stem cells ameliorate chronic experimental autoimmune encephalomyelitis. Stem Cells 27:2624-35.

Cross AK, Woodroofe MN. 1999. Chemokines induce migration and changes in actin polymerization in adult rat brain microglia and a human fetal microglial cell line in vitro. J Neurosci Res 55:17-23.

Cunningham C, Wilcockson DC, Campion S, Lunnon K, Perry VH. 2005. Central and systemic endotoxin challenges exacerbate the local inflammatory response and

increase neuronal death during chronic neurodegeneration. J Neurosci 25(40):9275-84.

Erblich B, Zhu L, Etgen AM, Dobrenis K, Pollard JW. 2011. Absence of colony stimulation factor-1 receptor results in loss of microglia, disrupted brain development and olfactory deficits. PLoS One 6:e26317

Estrach S, Schmidt S, Diriong S, Penna A, Blangy A, Fort P, Debant A. 2002. The human Rho-GEF trio and its target GTPase RhoG are involved in the NGF pathway, leading to neurite outgrowth. Curr Biol 12:307-312.

Giulian D, Ingeman JE. 1998. Colony-stimulating factors as promoters of ameboid microglia. J Neurosci 8:4707–4717.

Gonzalez-Rey E, Gonzalez MA, Varela N, O'Valle F, Hernandez-Cortes P, Rico L, Büscher D, Delgado M. 2010. Human adipose-derived mesenchymal stem cells reduce inflammatory and T cell responses and induce regulatory T cells in vitro in rheumatoid arthritis. Ann Rheum Dis 69:241-248.

Hanisch UK, Kettenmann H. 2007. Microglia: active sensor and versatile effector cells in the normal and pathologic brain. Nat Neurosci 10:1387-1394.

Hawkins PT, Anderson KE, Davidson K, Stephens LR. 2006. Signalling through Class I PI3Ks in mammalian cells. Biochem Soc Trans 34:547-662.

Huber AB, Kolodkin AL, Ginty DD, Cloutier JF. 2003. Signaling at the growth cone: ligand-receptor complexes and the control of axon growth and guidance. Annu Rev Neurosci 26:509-563.

Jonas RA, Yuan TF, Liang YX, Jonas JB, Tay DK, Ellis-Behnke RG. 2012. The spider effect: morphological and orienting classification of microglia in response to stimuli in vivo. PLoS One 7:e30763.

Karperien A, Ahammer H, Jelinek HF. 2013. Quantitating the subtleties of microglial morphology with fractal analysis. Front Cell Neurosci 7:3.

Kettenmann H, Hanisch UK, Noda M, Verkhratsky A. 2011. Physiology of microglia. Physiol Rev 91(2):461-553.

Kim YJ, Park HJ, Lee G, Bang OY, Ahn YH, Joe E, Kim HO, Lee PH. 2009. Neuroprotective effects of human mesenchymal stem cells on dopaminergic neurons through anti-inflammatory action. Glia 57:13-23.

Liu W, Brosnan CF, Dickson DW, Lee SC. 1994. Macrophage colony-stimulating factor mediates astrocyte-induced microglial ramification in human fetal central nervous system culture. Am J Pathol 145:48–53.

Lo AS, Taylor JR, Farzaneh F, Kemeny DM, Dibb NJ, Maher J. 2008. Harnessing the tumour-derived cytokine, CSF-1, to co-stimulate T-cell growth and activation. Mol Immunol 45:1276-1287.

Martin S, Vincent J-P, Mazella J. 2003. Involvement of the neurotensin receptor-3 in the neurotensin-induced migration of human microglia. J Neurosci 23:1198-1205.

Mosser DM, Edwards JP. 2008. Exploring the full spectrum of macrophage activation. Nat Rev Immunol 8:958-969.

Munder M. 2009. Arginase: an emerging key player in the mammalian immune system. Br J Pharmacol 158:638–651.

Perry VH, Nicoll JA, Holmes C. 2010. Microglia in neurodegenerative disease. Nat Rev Neurol 6(4):193-201.

Phinney DG, Prockop DJ. 2007. Concise review: mesenchymal stem/multipotent stromal cells: the state of transdifferentiation and modes of tissue repair--current views. Stem Cells 25:2896-2902.

Pixley FJ. 2012. Macrophage Migration and Its Regulation by CSF-1. Int J Cell Biol 2012:501962.

Pixley FJ, Stanley ER. 2004. CSF-1 regulation of the wandering macrophage: complexity in action. Trends Cell Biol 14:628-638.

Ridley AJ. 2011. Life at the leading edge. Cell 145:1012-1022.

Rossman KL, Der CJ, Sondek J. 2005. GEF means go: turning on RHO GTPases with guanine nucleotide-exchange factors. Nat Rev Mol Cell Biol 6:167-180.

Sampaio NG, Yu W, Cox D, Wyckoff J, Condeelis J, Stanley ER, Pixley FJ. 2011. Phosphorylation of CSF-1R Y721 mediates its association with PI3K to regulate macrophage motility and enhancement of tumor cell invasion. J Cell Sci 124:2021-2031.

Smith SD, Jaffer ZM, Chernoff J, Ridley AJ. 2008. PAK1-mediated activation of ERK1/2 regulates lamellipodial dynamics. J Cell Sci 121:3729-3736.

Soltys Z, Ziaja M, Pawlinski R, Setkowicz Z, Janeczko K. 2001. Morphology of reactive microglia in the injured cerebral cortex. Fractal analysis and complementary quantitative methods. J Neurosci Res 63(1):90-7.

Song S, Zhou F, Chen WR. 2012. Low-level laser therapy regulates microglial function through Src-mediated signaling pathways: implications for neurodegenerative diseases. J Neuroinflammation 9:219.

Tarassishin L, Suh HS, Lee SC. 2011. Interferon regulatory factor 3 plays an anti-inflammatory role in microglia by activating the PI3K/Akt pathway. J Neuroinflammation 8:187.

Uccelli A, Benvenuto F, Laroni A, Giunti D. 2011. Neuroprotective features of mesenchymal stem cells. Best Pract Res Clin Haematol 24:59-64.

Uccelli A, Prockop DJ. 2010. Why should mesenchymal stem cells (MSCs) cure autoimmune diseases? Curr Opin Immunol 22:768-774.

Wegiel J, Wisniewski HM, Dziewiatkowski J, Tarnawski M, Kozielski R, Trenkner E, Wiktor-Jedrzejczak W. 1998. Reduced number and altered morphology of microglial cells in colony stimulating factor-1-deficient osteopetrotic op/op mice. Brain Res 804:135–139.

Wilms H, Hartmann D, Sievers J. 1997. Ramification of microglia, monocytes and macrophages in vitro: influences of various epithelial and mesenchymal cells and their conditioned media. Cell Tissue Res 287:447-58.

Zappia E, Casazza S, Pedemonte E, Benvenuto F, Bonanni I, Gerdoni E, Giunti D, Ceravolo A, Cazzanti F, Frassoni F, Mancardi G, Uccelli A. 2005. Mesenchymal stem cells ameliorate experimental autoimmune encephalomyelitis inducing T-cell anergy. Blood 106:1755-61.

Zhang J, Li Y, Chen J, Cui Y, Lu M, Elias SB, Mitchell JB, Hammill L, Vanguri P, Chopp M. 2005. Human bone marrow stromal cell treatment improves neurological functional recovery in EAE mice. Exp Neurol 195:16-26.

Zhou C, Zhang C, Chi S, Xu Y, Teng J, Wang H, Song Y, Zhao R. 2009. Effects of human marrow stromal cells on activation of microglial cells and production of inflammatory factors induced by lipopolysaccharide. Brain Res 1269:23-30.

Figure legends

Figure 1. Adipose tissue-derived mesenchymal stem cells (ASC) induce cell shape changes in microglia. (A) Microglia cells were incubated in control medium (medium) or activated with LPS in the absence or presence of ASCs (in transwell inserts). When indicated, microglia were incubated with conditioned medium (CM) collected from ASC cultures. After 48 h incubation, cells were fixed and immunostained for the microglia marker CD11b. Similar results were obtained after 72 h incubation. Quantification of the cell shape was performed by calculating the form factor = 4π*area/(perimeter). **(B)** Microglia were incubated for 24 h with LPS and then incubated with control culture medium (medium) or ASC-conditioned medium (CM) for further 24 h. Cells were CD11b-immunostained and the form factor was calculated in both conditions. Data are mean±SEM and 102 to 212 cells per condition in at least three independent experiments were quantified. **p<0.01, ***p<0.001. Scale bars, 50 μm in left panel pictures and 10 μm in right panel pictures, for each treatment.

Figure 2. Microglia cell shape changes induced by ASCs depend on the production of CSF-1. Microglia cells were incubated in control medium (medium), with ASCs (in transwell inserts) or with conditioned medium (CM) collected from ASC cultures in the absence or presence of neutralizing antibodies against IL-6 or CSF-1. When indicated, recombinant CSF-1 (10 ng/ml) was added to microglia cultured with control medium. After 48 h of culture, cells were CD11b-immunostained and the cell shape was quantified by calculating the form factor in all conditions. Data are mean±SEM, and 107 to 249 cells per condition in at least three independent experiments were quantified. *p<0.05, **p<0.01, ***p<0.001 vs. medium; $^{\#}$p<0.05, $^{\#\#\#}$p<0.001. Scale bars, 50 μm.

Figure 3. Microglia induced by ASC show non-inflammatory, neuroprotective properties and increased phagocytic capacity. (A) and **(B)** Microglia cells were incubated in control medium (medium) or in conditioned medium (CM) collected from ASC cultures in the absence or presence of LPS. After 24 h, gene expression for IL6 and TNFα was quantified by qRT-PCR and normalized to β-actin levels. Culture supernatants were assayed for the content of TNFα using a specific ELISA. Results are expressed as relative amount to microglia treated with control medium. Data are mean±SEM of three (for TNFα ELISA) four (for TNFα qRTPCR) or five (for IL-6) independent experiments. *p<0.05, **p<0.01, ***p<0.001. **(C)** and **(D)** Microglia cells were incubated in control medium or in CM. After 24 h, gene expression for BDNF, GDNF, FGF2 and ADNP was quantified by qRT-PCR and normalized to β-actin levels. Protein expression for BDNF and ADNP was determined by Western blot analysis and normalized to α-tubulin levels. Results are expressed as fold-change to microglia treated with control medium (dashed line in **C**). Data are mean±SEM of three independent experiments. *p<0.05, **p<0.01. **(E)** Microglia cells were incubated in control medium or in CM, or co-incubated in transwells with ASC in the absence or presence of LPS. At the indicated times, the protein expression of Arginase-1 was determined by Western blot analysis. Quantification corresponds to 48 h cultures and is expressed in arbitrary units (AU). Data are mean±SEM of four independent experiments. *p<0.05, **p<0.01. **(F)** Microglia were cultured in control medium, with ASCs (in transwell inserts) or in CM for 48 h and then subjected to a phagocytosis assay using fluorescent Nile Red FluoSpheres. Data are the mean±SEM of three independent experiments with 281 to 423 cells being analyzed per condition. The quantification shows the percentage of cells in the culture that did not phagocyte (0

beads) or phagocytosed few (1-5 beads) or many (>6 beads) microspheres. Scale bars, 50 μm. *p<0.05, **p<0.01, ***p<0.001.

Figure 4. Signalling molecules activated upon ASC CM treatment. Microglia cells were incubated in control medium (medium) or in ASC conditioned medium (CM) in the absence or presence of LPS at the indicated time points. The time point at 0 min corresponds to cells growing in microglia growth medium. **(A)** After 5 min of incubation, the activation of Akt and ERK1/2 was assayed by quantifying the levels of phosphorylated-Akt and phosphorylated-ERK1/2 by Western blot analysis, expressed as arbitrary units (AU) normalized to total Akt and ERK1/2, respectively. Data are mean±SEM of three independent experiments. *p<0.05, **p<0.01, ***p<0.001 **(B)** and **(C)** At the indicated time points, cell lysates were assayed for the activation of the small RhoGTPases Rac1 and Cdc42 as described in Materials and Methods and normalized to total Rac1 and Cdc42 amounts in cell lysates. Data are mean±SEM of three independent experiments. *p<0.05.

Figure 5. Activation of PI3K/Akt, Cdc42 and Rac1 are involved in the ASC-induced microglia cell shape changes. (A) Microglia cells were incubated in control medium (medium) or in ASC-conditioned medium (CM) containing DMSO in the absence or presence of the PI3K inhibitor LY 294002 (10 μM) or the MEK inhibitor PD 98059 (50 μM) for 24 h. Then cell shape was analyzed by CD11b-immunostaining and quantified by calculating the form factor. Data are mean±SEM of four independent experiments, with 106 to 131 cells being analyzed for each condition. **p≤0.01. Scale bars, 50 μm. **(B)** GFP-tagged wild type (wt) and dominant negative (DN) mutants of Cdc42 and Rac1 were nucleofected into microglia cells and then treated with ASC-

conditioned medium (CM) for 48h. Cell shape changes were analyzed by CD11b-immunostaining and quantified by calculating the form factor. Data are mean±SEM of four independent experiments, with 45 to 69 cells being analyzed for each mutant. Scale bars, 10 μm for RhoGTPases and 50 μm for GFP. **p<0.01; ***p<0.001.

Figure 1

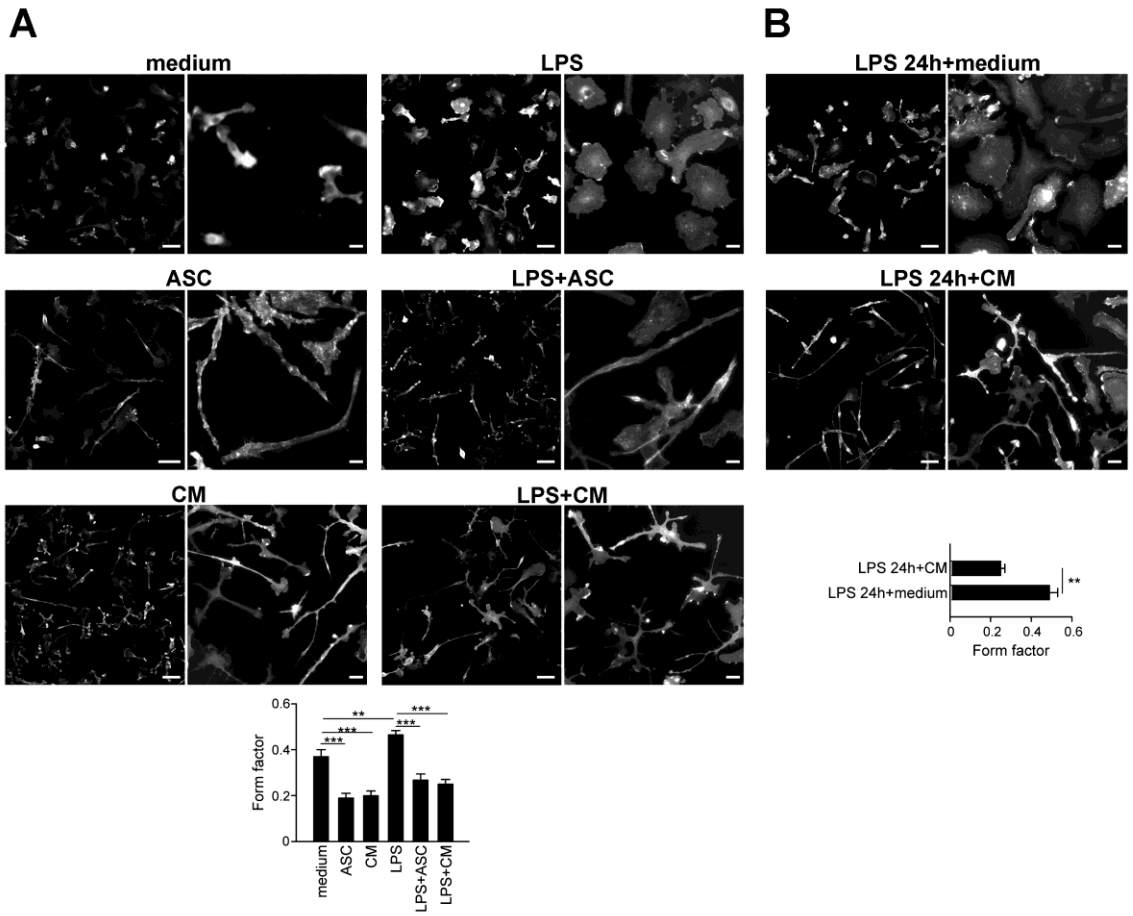
A
medium
LPS
ASC
LPS+ASC
CM
LPS+CM
B
LPS 24h+medium
LPS 24h+CM
LPS 24h+CM
LPS 24h+medium
**
0
0.2
0.4
0.6
Form factor
Form factor
0.6
0.4
0.2
0
**
***
***
***
***
medium
ASC
CM
LPS
LPS+ASC
LPS+CM

Figure 2

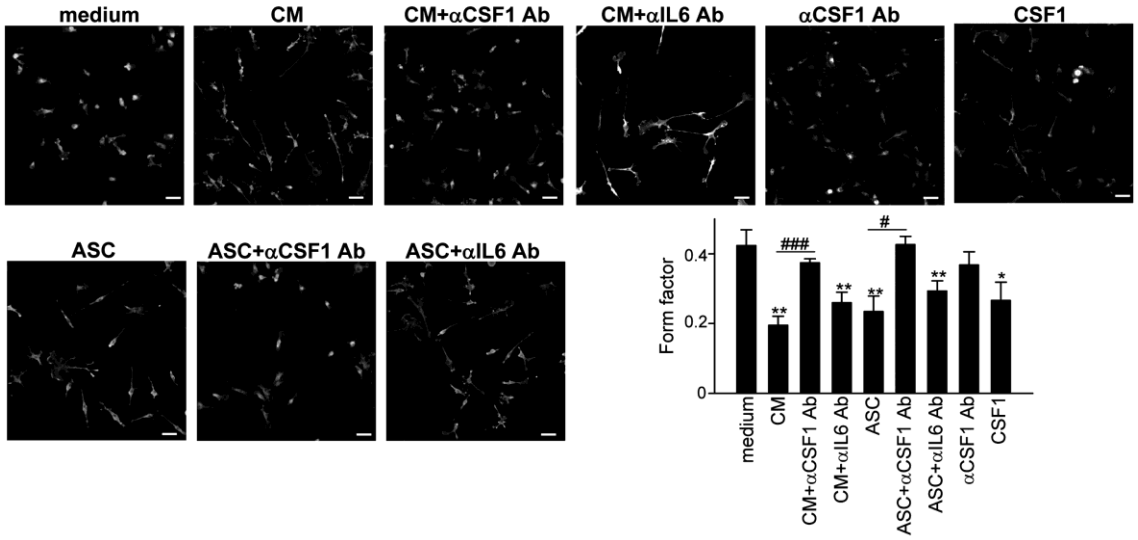
medium
CM
CM+αCSF1 Ab
CM+αIL6 Ab
αCSF1 Ab
CSF1
ASC
ASC+αCSF1 Ab
ASC+αIL6 Ab
Form factor
0.4
0.2
0
###
#
**
**
**
**
**
*
medium
CM
CM+αCSF1 Ab
CM+αIL6 Ab
ASC
ASC+αCSF1 Ab
ASC+αIL6 Ab
αCSF1 Ab
CSF1

Figure 3

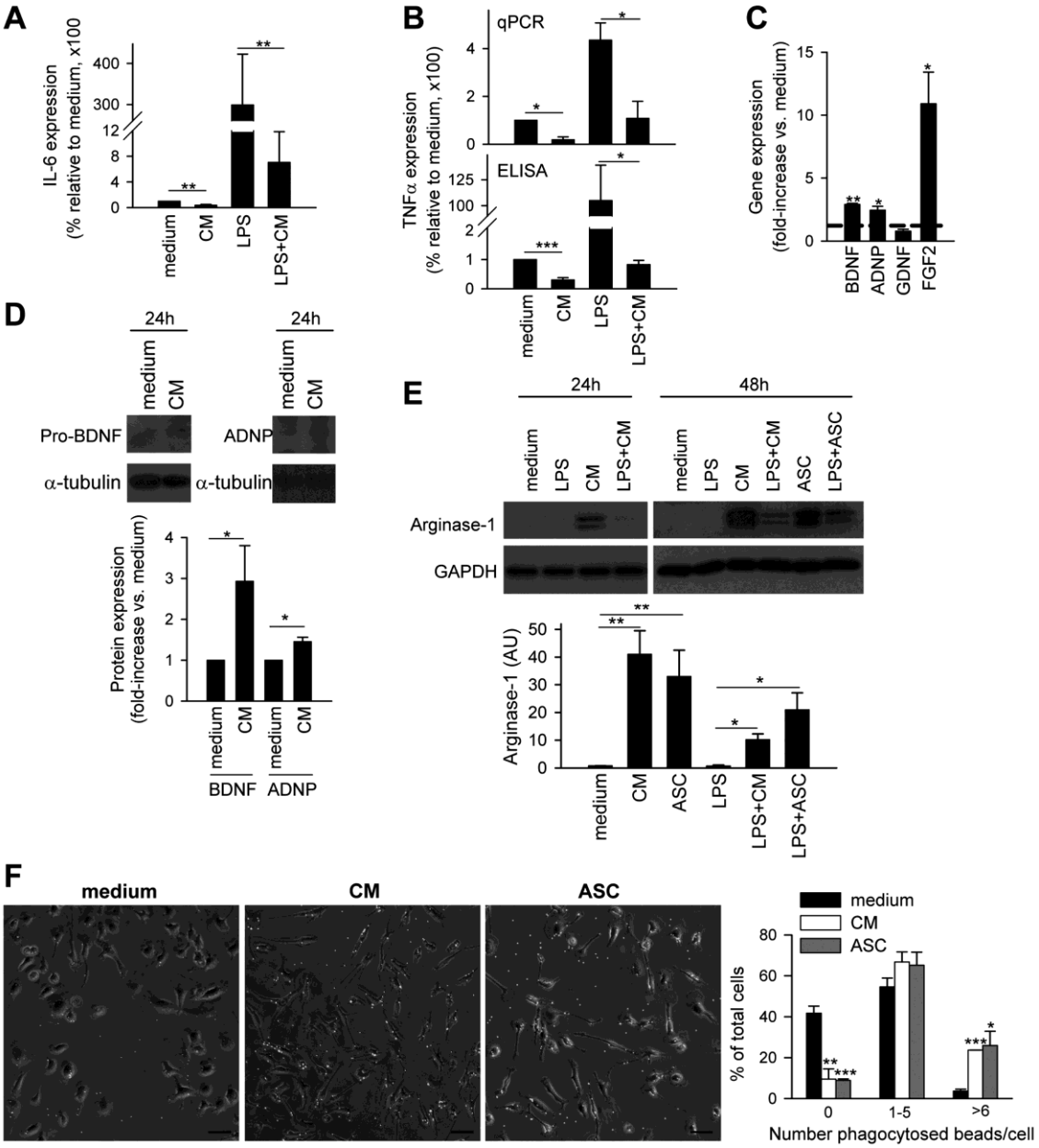
A
IL-6 expression (% relative to medium, x100)
medium
CM
LPS
LPS+CM
B
qPCR
ELISA
TNFα expression (% relative to medium, x100)
C
Gene expression (fold-increase vs. medium)
BDNF
ADNP
GDNF
FGF2
D
24h
Pro-BDNF
ADNP
α-tubulin
Protein expression (fold-increase vs. medium)
BDNF
ADNP
E
24h
48h
Arginase-1
GAPDH
Arginase-1 (AU)
ASC
LPS+ASC
F
medium
CM
ASC
% of total cells
Number phagocytosed beads/cell

Figure 4

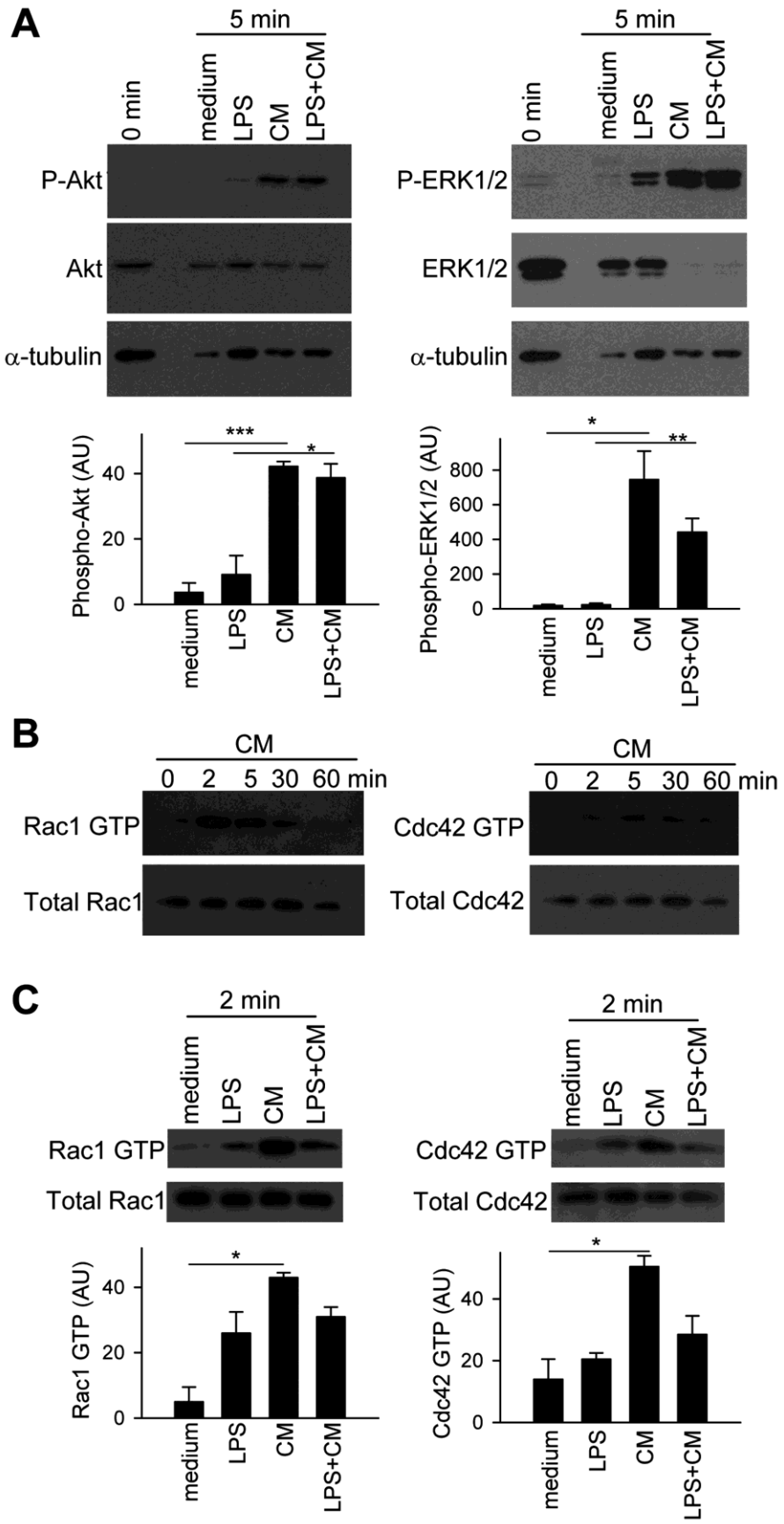
A
5 min
0 min
medium
LPS
CM
LPS+CM
P-Akt
Akt
α-tubulin
P-ERK1/2
ERK1/2
α-tubulin
Phospho-Akt (AU)
Phospho-ERK1/2 (AU)
***
*
**
B
CM
0 2 5 30 60 min
Rac1 GTP
Total Rac1
Cdc42 GTP
Total Cdc42
C
2 min
Rac1 GTP
Total Rac1
Cdc42 GTP
Total Cdc42
Rac1 GTP (AU)
Cdc42 GTP (AU)

Figure 5

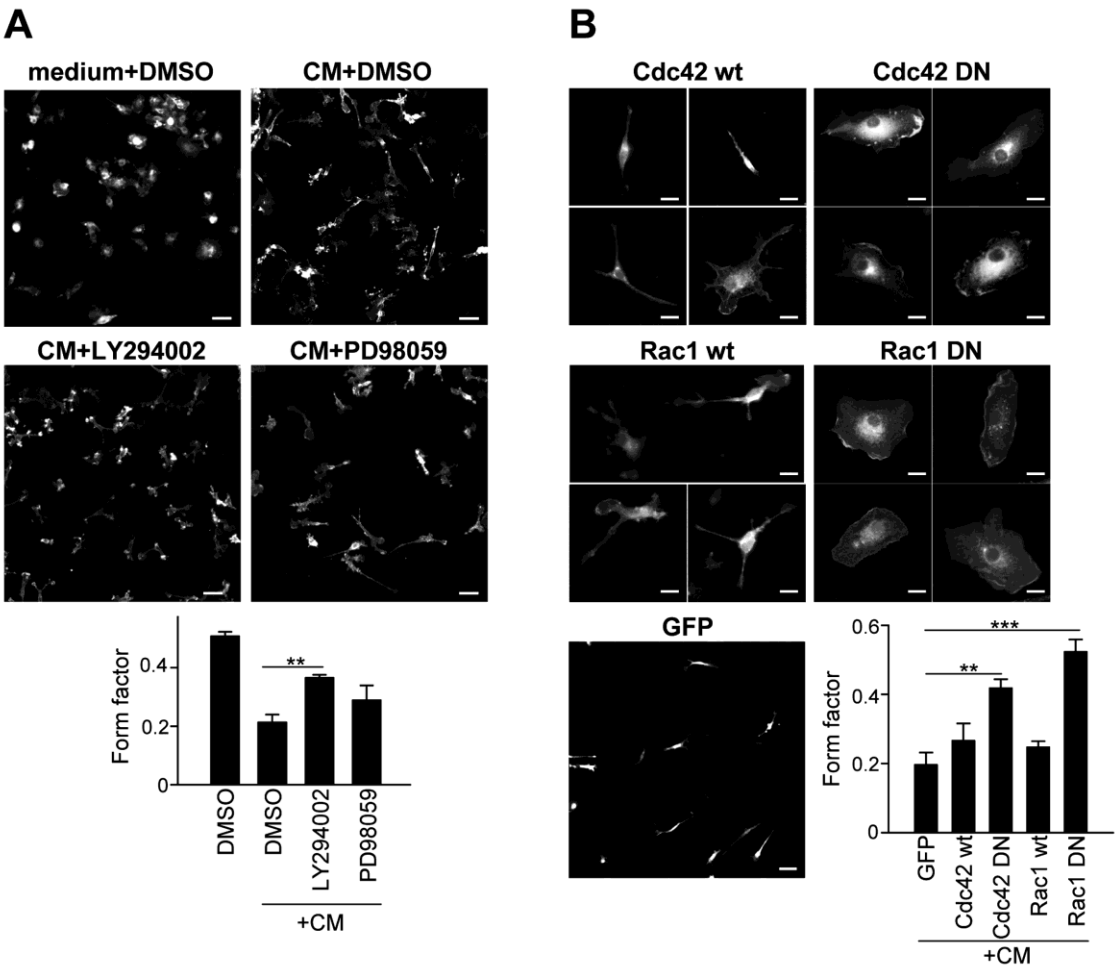
A
medium+DMSO
CM+DMSO
CM+LY294002
CM+PD98059
Form factor
0.4
0.2
0
**
DMSO
DMSO
LY294002
PD98059
+CM
B
Cdc42 wt
Cdc42 DN
Rac1 wt
Rac1 DN
GFP
Form factor
0.6
0.4
0.2
0
***
**
GFP
Cdc42 wt
Cdc42 DN
Rac1 wt
Rac1 DN
+CM